

Article

Performance of Parabolic Trough Collector with Different Heat Transfer Fluids and Control Operation

Surender Kannaiyan ¹ and Neeraj Dhanraj Bokde ^{2,3,*} 

¹ Department of Electronics and Communication, Visvesvaraya National Institute of Technology, Nagpur 440010, India

² Center for Quantitative Genetics and Genomics, Aarhus University, 8000 Aarhus, Denmark

³ iCLIMATE Aarhus University Interdisciplinary Centre for Climate Change, Foulum, 8830 Tjele, Denmark

* Correspondence: neerajdhanraj@qgg.au.dk

Abstract: Electricity generation from solar energy has become very desirable because it is abundantly available and eco-friendly. Mathematical modeling of various components of a Solar Thermal Power plant (STP) is warranted to predict the optimal and efficient operation of the plant. The efficiency and reliability of STPs are maximized based on different operating strategies. Opting for proper Heat Transfer Fluid (HTF), which is proposed in this paper, helps in reducing operating complexity and lowering procurement cost. The Parabolic Trough Collector (PTC) is the heart of STP, where proper focusing of PTC towards solar radiation is the primary task to maximize the outlet temperature of HTF. This maximum temperature plays a major factor due to diurnal solar radiation variation, and its disturbance nature, with the frequent startup and shutdown of STP, is avoided. In this paper, the PTC component is modeled from the first principle, and, with different HTF, the performance of PTC with constant and quadratic solar disturbances is analyzed along with classical control system designs. Through this, the operator will be able to choose proper HTF and resize the plant components depending on plant location and weather conditions. Furthermore, the thermal energy is collected for therminol oil, molten salt, and water; and its performance with different inputs of solar radiation is analyzed along with closed-loop controllers. Thermal energy extracted by therminol oil, molten salt, and water with constant solar radiation results in 81.7%, 73.7% and 18.7%, respectively.

Keywords: solar thermal power plant; parabolic trough collector; heat transfer fluid; classical control system



Citation: Kannaiyan, S.; Bokde, N.D. Performance of Parabolic Trough Collector with Different Heat Transfer Fluids and Control Operation. *Energies* **2022**, *15*, 7572. <https://doi.org/10.3390/en15207572>

Academic Editor: Noam Lior

Received: 9 September 2022

Accepted: 9 October 2022

Published: 14 October 2022

Publisher's Note: MDPI stays neutral with regard to jurisdictional claims in published maps and institutional affiliations.



Copyright: © 2022 by the authors. Licensee MDPI, Basel, Switzerland. This article is an open access article distributed under the terms and conditions of the Creative Commons Attribution (CC BY) license (<https://creativecommons.org/licenses/by/4.0/>).

1. Introduction

Among all the renewable energy resources available, solar energy has been of great interest to researchers and industrialists. Kalogirou [1] described the environmental problems of fossil fuels. In addition, different types of solar collectors, their construction, functionality, thermal analysis, and applications were also presented. Solar Thermal Power (STP) plants make use of solar radiation to provide heat to a thermodynamic cycle through a heat exchanger, in which two fluid streams come into thermal contact to transfer heat from primary to secondary fluid. The secondary fluid is used to drive a turbine generator to produce electricity.

A solar collector is a key element in the solar thermal energy system. It captures the incoming solar radiation and converts it into a usable form, transforming the collected heat in the collector array into electricity as efficiently as possible through increasing the upper process temperature for the conversion. The quality of components and systems in STP is a decisive criterion in achieving greater efficiencies and reducing costs. Researchers are therefore working on suitable measurement methods and devices in order to measure the quality and subsequently improve the weak points. Predominantly, therminol oil is used as Heat Transfer Fluid (HTF) in Parabolic Trough Collector (PTC), and its operating temperature of thermal oil is limited to just under 400 °C [2].

In literature, PTC consists of parabolic reflectors as concentrators, rays to be focussed on the focal line and provided with a single axis tracking mechanism with East to West or North to South tracking with reliable, commercially proven, and mature technology. Modularity, scalability and storage pave the way for large heat production, being cost effective as compared with central receiver and parabolic dish technologies. Essential qualities for a Heat Transfer Fluid (HTF) to be used as a working fluid in PTC are high thermal capacity and superior conductivity with a minimum coefficient of thermal expansion. It should be less viscous, with no corrosive behavior or toxicity, and thermally and chemically stable. The desired properties should be unaffected during the entire range of operating conditions and long durations. Apart from therminol oil, molten salt, water and nanofluids have excellent stability. Currently, there is no practical implementation studies of thermal enhancement in these nanofluids [3]. PTC with therminol oil as the heat transfer medium is among the most widely used [4]. A Linear Fresnel Reflector (LFR) type solar collector with water as HTF to generate direct steam generation, which does not require a separate Heat Exchanger (HX) block for generation of steam, is used as an alternative—whereas LFR has low efficiencies, affected by heavy disturbances such as wind velocity, cloud cover, shadowing, among others [5]. Saucedo et al. [6] showed that the thermal efficiency of PTC is 15% higher than LFR.

Camacho et al. [7] developed a PTC mathematical model using the energy balance for therminol oil as a fluid and absorber pipe energy balance alone. Powell et al. [8] developed a PTC mathematical model with an additional energy balance for a glass pipe by considering a few realistic losses compared to the model proposed by Camacho et al. [7]. Using a Powell et al. [8] dynamic model, Kannaiyan et al. [9] validated the model with real plant data from a 1MWe gurgaon plant [10]. Silva et al. [11] presented a study on HTF as a therminol oil temperature profile of PTC that was modeled using a transport equation and solution obtained using the method of characteristics. Camacho et al. [12] described several control system designs using data-driven models for PTC.

Molten salt as HTF had the benefit of lower procurement cost, and operating at a higher temperature (565 °C) [13]. Molten salt has already proved itself as a storage medium on a commercial scale [4]. Using molten salt as HTF with a hybrid adaptive-control scheme and a time-warped predictive controller, the outlet temperature of molten salt is controlled for intermittent solar radiation [13].

PTC with water as HTF is called Direct Steam Generation (DSG). The DSG is comprised of several advantages such as it is inexpensive since it eliminates extra cost of the heat exchanger and it does not use hazardous chemicals. In addition, It is non-corrosive [14]. Yan et al. [15] used PTC with water as HTF and developed a dynamic model with three differential equations for the temperature of the water, pipe, and glass profiles, which are analyzed without describing the momentum equation. Several researchers have developed a dynamic model for DSG as a set of Differential-Algebraic Equations (DAEs) [16–18]. In this study, there is no two-phase steam generation that occurs, pertaining to solar radiation excitation.

Chatoorgoon [14] developed stability studies for homogeneous two-phase flow, which works efficiently for both small-time and large-time steps. Odeh et al. [19] analyzed a two-phase flow model using single-phase and two-phase Heat Transfer Coefficient (HTC) correlation coefficients used in DSG.

Recent innovation on design on PTC with a double U-tube sun-tracked with HTF is modeled using an energy balance equation along a numerical scheme for computation grid length, and experimental validation is discussed in detail in [20]. Furthermore, a rotating absorber tube and its thermal variable performance are discussed in [21]. Maintaining HTF outlet temperature by regulating the mass flow rate is essential in improving plant efficiency [22]. Similarly, cyclic startup and shutdown of STP can also be regulated [23].

To avoid such cyclic startup and shutdown in STP, PTC outlet temperature is regulated through control system design. PTC dynamic modelling and control studies help to reduce the operating cost in different disturbances such as wind speed and the temperature of

HTF flowing in. Solar radiation on PTC is not predictable due to cloud cover, and the temperature of HTFs coming into the PTC is not constant. By maintaining HTFs' outlet temperature at setpoint, better performance of PTC assistance to enhance electric power generation in STP is achieved. Setpoint of HTF's outlet temperature is maintained by manipulating the HTF's flow rate through PTC. To maintain HTF outlet temperature of PTC at a desired setpoint, irrespective of disturbances, along with the heat gain gradient of HTF also being maintained within limits to avoid thermal losses and oil leakage, it is essential for the safe operation of STP [7,24]. Furthermore, it also helps to find the best operating strategies to produce maximum electricity generation.

In several literature works, this has been chosen as a control and manipulated variable with several controller techniques such as PID, FeedForward [25,26] feedback linearization, Fuzzy, GPC, gain scheduling [7,25], among others. Predictive functional control and PI control for PTC with therminol oil with different solar disturbance and its performance are studied [27].

Direct steam generation is obtained using a mass flow rate of water flow as manipulated variables in PTC [17]. Using a PI controller, linear transfer function steam outlet temperature is controlled [28]. A brief review on controller methods implemented on direct steam generation is discussed [29].

The aim of the present study is to construct a dynamic model of a PTC for various HTFs with therminol oil, molten salt, and water; and then analyze their performances in different scenarios, such as heat gain performance. The purpose of this paper is to fill the research gap of utilizing the performance of alternative HTFs, molten salt, and water, for PTC and to compare with therminol oil. While comparing these HTFs, transient simulation with different disturbance fluctuation is explored along with relevant classical control action. The methodology followed in this paper is discussed as follows: the design of controller within their limits and physical reliability is essential. Thus, the design of a proper control system needs four sequences of steps as follows: (1) Using a validated dynamic model of PTC [9], step input is applied on its manipulated variable; (2) Process Variable (PV) data are collected; (3) Best fit Transfer function is obtained through a MATLAB system identification toolbox; (4) Controller tuning parameters are obtained based on fitted transfer function and IMC tuning rules; (5) Solar and thermal energy extraction for different HTFs, and its controller performance is studied.

The remaining sections of this paper are organized as follows: Section 2 presents the modeling of parabolic trough collector, and the control structure design of PTC is discussed in Section 3. In Section 4, case studies of HTFs are discussed, followed by conclusions in Section 5.

2. Modeling of a Parabolic Trough Collector

Modeling of a Parabolic Trough Collector (PTC) obtained on the basis of conservation of energy in a finite volume for each of its three components, named HTF, absorber pipe, and glass envelope. The dynamics of these three components are closely related to one another [8]. The glass tube is used to reduce the convective loss from the receiver tube by transmitting 90% of incoming short wave solar radiation while not transmitting the emitted longwave radiation outward by an absorber tube [1].

2.1. PTC with HTF

The dynamic model of PTC consists of three Partial Differential Equations (PDEs), one each for HTF, absorber pipe, and glass envelope. In the PTC modeling, all the significantly dominant factors are taken into consideration. The schematic of PTC with HTF as therminol oil and molten salt is shown in Figure 1.

Energy balance of HTF of PTC is obtained as (1):

$$\frac{\partial T_o}{\partial t} (\rho_o C_{p,o} A_A) = \dot{m}_o C_{p,o} \frac{\partial T_o}{\partial x} + h_p p_{Ai} (T_A - T_o) \tag{1}$$

Energy balance for absorber pipe of PTC is obtained as (2):

$$\rho_A C_A A_A \frac{\partial T_A}{\partial t} = h_p p_{Ai} (T_o - T_A) - \frac{\sigma}{\frac{1}{\xi_A} \frac{1-\xi_E}{\xi_E} \left(\frac{r_{Ao}}{r_{Ei}}\right)} p_{Ao} (T_A^4 - T_E^4) + I\eta_{opt} W \tag{2}$$

Energy balance for glass envelope is obtained as (3):

$$\rho_E C_E A_E \frac{\partial T_E}{\partial t} = \frac{\sigma}{\frac{1}{\xi_A} \frac{1-\xi_E}{\xi_E} \left(\frac{r_{Ao}}{r_{Ei}}\right)} p_{Ai} (T_A^4 - T_E^4) - \sigma p_{Eo} \xi_E (T_E^4 - T_{sky}^4) - h_{air} p_{Eo} (T_E - T_{air}) \tag{3}$$

The PDEs are converted into Ordinary Differential Equations (ODEs) using the backward finite difference method. The number of necessary grid points for the computation is obtained by its successive increment and tracking the consequent change in the temperature until the change is less than the prescribed level. Based on the analysis, a total of 15 grid points are found to be necessary for a PTC of 500 m long. The number of state variables present in PTC for therminol oil and molten salt is 45 (i.e., 15 × 3) and derivatives of the states are integrated over time. The details of mathematical modeling of PTC with therminol oil as HTF and its discretization, grid point computation, validation with real plant data, and implementation numerical scheme are discussed in detail by Kannaiyan et al. [9].

The proposed PTC model uses therminol oil and molten salt, and the pressure loss in both cases is negligible. Therminol oil and molten salt thermodynamic properties are obtained as shown in Appendix A. However, in the case of water as HTF, the pressure loss from input to output of PTC is significant due to the occurrence of the two-phase generation. The computation variables and its schematic, and its simulation approach for PTCTHO, PTCMS and PTCWAT are shown in Figures 2 and 3.

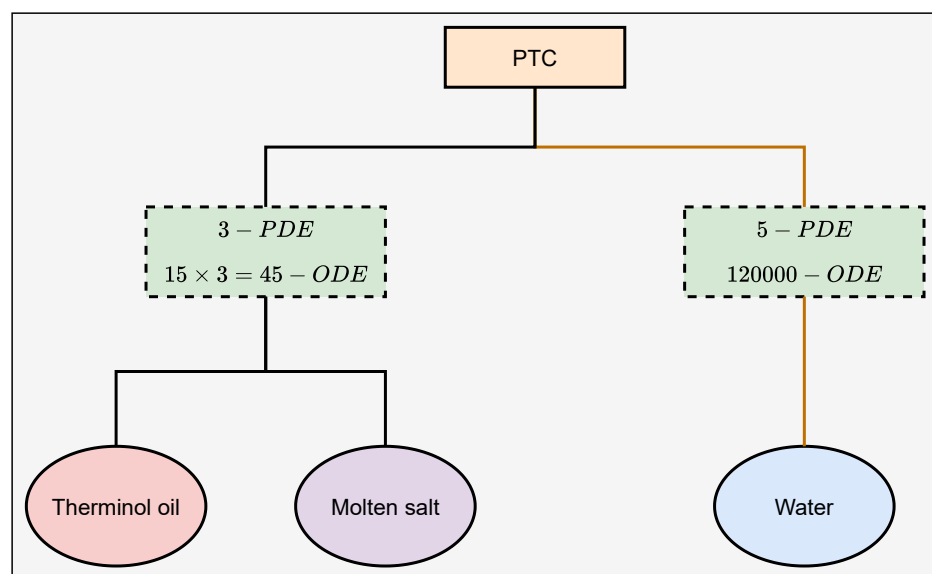


Figure 2. PTC with different HTF mathematical modeling analysis.

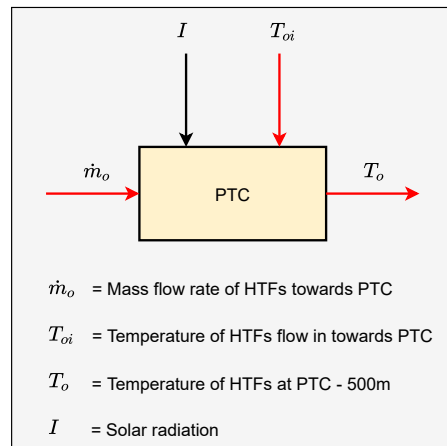


Figure 3. PTC schematic (open-loop configuration).

2.2. Parabolic Trough Collector with Water as HTF (PTCWAT)

Dynamic simulation of PTCWAT is obtained using Chatoorgoon's model [14] that discusses the conservation of mass, momentum, and energy (Equations (4) to (6)) with a discretization scheme. In the energy Equation (6), term q_w captures the heat energy supplied from solar energy [9]. In addition, Equations (2) to (3) are also considered, which carry HTF to obtain the temperature increase of water at a total length of PTC at 500 m. Steam generation contributes to significant pressure loss that occurs with water as HTF, and it affects the energy output of PTC. Accounting for that dynamic model of PTCWAT consists of the following equations derived from first principles as [14]:

$$\text{Mass:} \quad \frac{\partial \rho}{\partial t} + \frac{\partial(\rho u)}{\partial x} = 0 \quad (4)$$

$$\text{Momentum:} \quad \frac{\partial(\rho u)}{\partial t} + \frac{\partial(\rho u^2)}{\partial x} + \frac{\partial P}{\partial x} + C_k \rho u^2 + \rho g = 0 \quad (5)$$

$$\text{Energy:} \quad \frac{\partial}{\partial t} \left[\left(\rho \left(h + \frac{u^2}{2} \right) \right) \right] + \frac{\partial}{\partial x} \left[\left(\rho u \left(h + \frac{u^2}{2} \right) \right) \right] + \rho u g = \frac{\partial P}{\partial t} + q_w \quad (6)$$

$$\text{State:} \quad \rho = f(P, h) \quad (7)$$

Energy balance for PTCWAT absorber pipe is obtained with (8):

$$\begin{aligned} \rho_A C_A A_A \frac{\partial T_A}{\partial t} = & h_p p_{Ai} (T_{(w/st/2\phi)} - T_A) - \frac{\sigma}{\frac{1}{\xi_A} + \frac{1-\xi_E}{\xi_E} \left(\frac{T_A}{T_E} \right)} p_{Ao} (T_A^4 - T_{sky}^4) \\ & + I_c \eta_{opt} W - h_{air} p_{Eo} (T_A - T_{air}) \end{aligned} \quad (8)$$

Energy balance for PTCWAT glass envelope is obtained with (9):

$$\begin{aligned} \rho_E C_E A_E \frac{\partial T_E}{\partial t} = & \frac{\sigma}{\frac{1}{\xi_A} + \frac{1-\xi_E}{\xi_E} \left(\frac{T_A}{T_E} \right)} p_{Ai} (T_A^4 - T_E^4) \\ & - \sigma p_{Eo} \xi_E (T_E^4 - T_{sky}^4) - h_{air} p_{Eo} (T_E - T_{air}) \end{aligned} \quad (9)$$

PTCWAT has one mass balance, three conservation equations (water, absorber tube and glass tube) and one momentum equation. The schematic of PTC with water as HTF is shown in Figure 4. In Appendix C, the relation of solar energy received per unit volume on an absorber pipe for sectional length for PTCWAT is discussed in detail. Parameters involved in PTCWAT are listed in Table A1 for Equations from (4) to (9).

In this simulation, PTCWAT consists of 'n' sections from its entire length, so the number of state variables present is given by the length of pipe multiplied with sections of pipe ($500 \times 50 \times 5 = 125,000$). The numerical solution used for solving the PTCWAT is

implicit Euler with a step size of time (dt) for 60 s [9]. Thermodynamic properties of water and steam are accessed from MATLAB library files Xsteam [30].

In PTC with water as HTF, the process variable is considered as enthalpy instead of the temperature of water flowing out. In the proposed case studies, the steam generation case does not occur, and it is possible, if there is an increase in optical efficiency of PTC or inlet input temperature of the water is increased, that steam generation occurs.

If direct steam generation occurs from the PTC, the temperature of the water is constant; however, the steam quality varies due to heat gain from the solar radiation. Steam quality is more at the end of exit; then, pressure loss occurs more with reference to input pressure applied at the input of PTC. This is one of the case studies discussed in this article and performed in Appendix D to realize the steam quality generation.

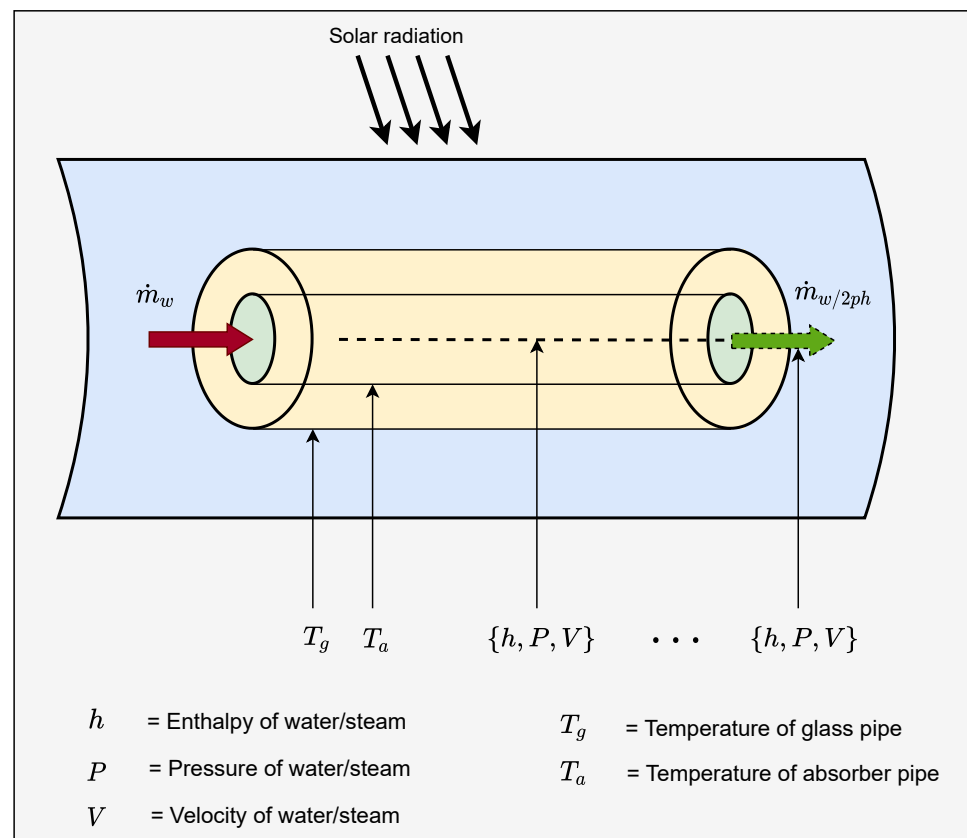


Figure 4. Parameters and dynamic variables of PTCWAT.

3. Control Structure Design for PTC

3.1. System Identification of PTC with HTFs

Development of linear system is obtained by choosing a specific operating point, exciting the Manipulated Variable (MV) through step input, and, through the response of the PTC process variable (PV), a suitable proxy model of PTC is obtained. Based on the obtained data order of the system, the nature of the transfer function is selected based on the complexity of controller design. In this study, First Order (FO) is selected based on sufficient fit percentage.

3.1.1. First Order (FO) Approximation

First Order (FO) is approximated with process gain (K_p) and time constant (τ). Process gain (K_p) is obtained based on the ratio of change in the magnitude of output (PV) to the change in magnitude of input (MV). The time constant (τ) is obtained by predicting the time taken for the output variable to reach 63% of change in the Process Variable (PV) to its steady-state value. PV responds to a change in manipulated variable [31], and it is

obtained as shown in (10). The parameters of the transfer function under consideration were obtained using the system identification toolbox in MATLAB 2012a; details of the best fit equation are discussed in Appendix E:

$$G(s) = \frac{K_p}{\tau s + 1} \quad (10)$$

The initial value assigned during this FO simulation for therminol oil and molten salt is as follows: Oil inlet temperature 200 °C, the flow rate of oil 3 kg/s, the initial temperature of absorber and glass are 201 °C and 40 °C, respectively. In the case of water inlet temperature set at 125 °C and the flow rate of oil 2 kg/s, the initial temperatures of absorber and glass are 126 °C and 40 °C, respectively. Table 2 shows other variables during the step test. The remaining parameters are set as per the design of PTC as shown in Table 1. Figure 5 shows the step test for PTC with therminol oil and molten salt as HTF by simulating Equations (1) to (3). Figure 6 shows the step test for PTC with water as HTF by simulating Equations (4) to (9). Based on Figure 6, the transfer function is fitted as shown in Table 3.

Using those identified transfer functions, controller tuning was obtained and utilized in the dynamic model of PTC for case study simulation.

Table 2. Step test inputs for system identification of PTC for HTFs.

	Input during Step Test				
	I (W/m ²)	η_{opt}	\dot{m}_o (Kg/s)	Manipulated Variable (MV)	Process Variable (PV)
PTCTHO	600	0.4	3 to 4	Mass flow rate of Therminol oil flow in towards PTC	Therminol oil outlet temperature
PTCMS	600	0.4	3 to 4	Mass flow rate of molten salt flow in towards PTC	Molten salt outlet temperature
PTCWAT	600	0.4	1 to 2	Mass flow rate of Water flow in towards PTC	Water outlet temperature

Table 3. Control parameters for different HTFs.

Parameters System	PTCTHO	PTCMS	PTCWAT
Manipulated variable (MV)	Therminol oil flow rate	Molten salt flow rate	Water flow rate
Process Variable (PV)	Therminol oil temperature flow out of PTC	Molten salt temperature flow out of PTC	Water temperature (steam enthalpy) flow out of PTC
Disturbance	Therminol oil inlet temperature, Solar radiation	Molten salt inlet temperature, Solar radiation	Water inlet temperature, Solar radiation
Approximation Model (S domain)	$\frac{-17}{360 s+1}$	$\frac{-21}{961 s+1}$	$\frac{-80}{360 s+1}$
Controller Tuning ($K_p; T_i$)	-0.107, 247	-0.142, 720	-0.0353, 270
Fit Percentage (%)	92.37	98.86	86.37

PTCTHO = Parabolic Trough Collector with therminol oil as heat transfer fluid; PTCMS = Parabolic trough collector with molten salt as heat transfer fluid; PTCWAT = Parabolic trough collector with water as the heat transfer fluid

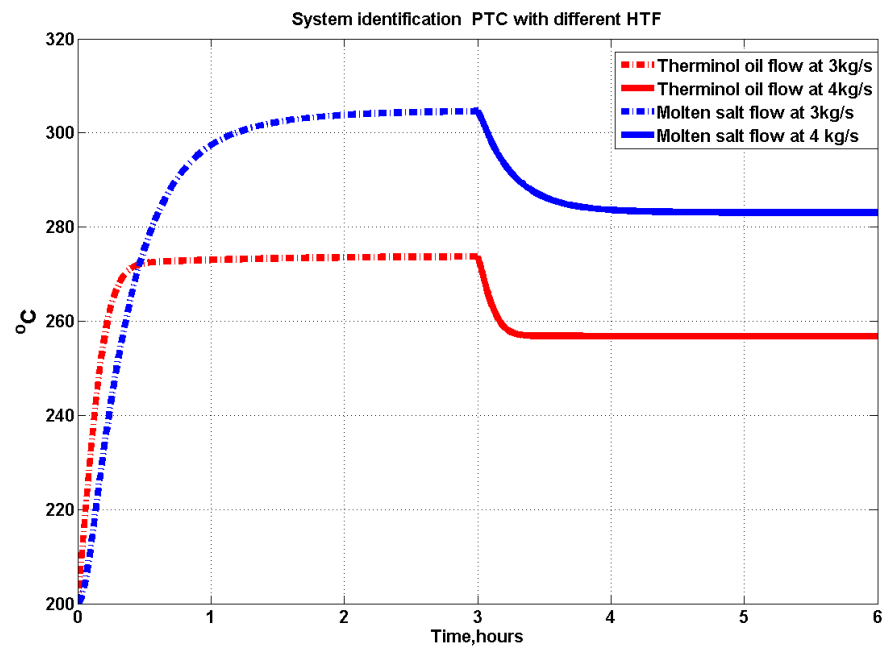


Figure 5. System identification of PTC for therminol oil and molten salt.

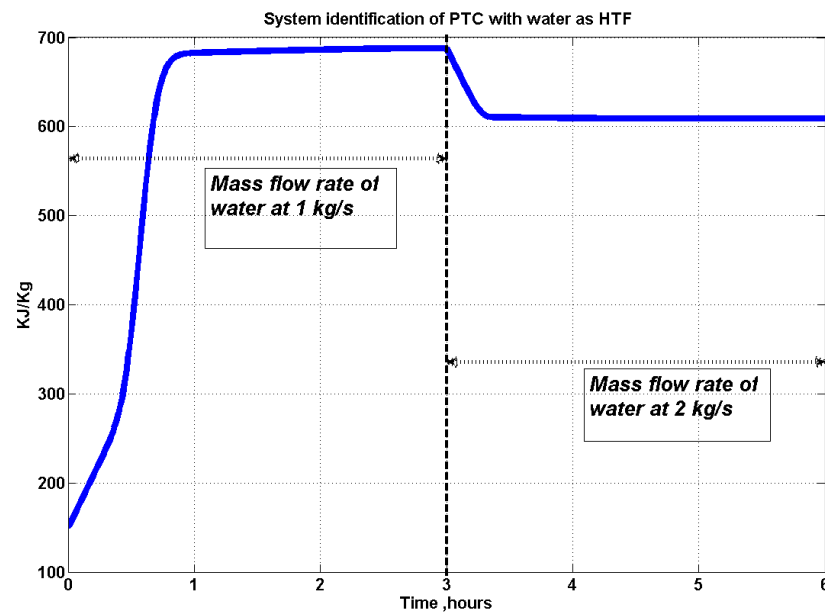


Figure 6. System identification of PTC for water as HTF.

3.2. Controller Tuning

Several tuning algorithms are available in the literature. The Internal Model Control (IMC) is employed for the PTC since it explicitly uses the desired closed-loop response and the specific form of the transfer function of the system used, in order to obtain the tuning parameters [31,32]. The various tuning rules to obtain K_c , τ_i , and τ_d , depending on the form of the transfer function used for the components of the STP, are outlined in Table 4.

Table 4. IMC—controller tuning rules.

G_P	G_{CL}	K_C	τ_i	τ_d
$\frac{K_P}{\tau s + 1}$ [31]	$\frac{\gamma s + 1}{\lambda s + 1}$	$\frac{2\tau - \lambda}{K_P \lambda}$	$\frac{2\tau\lambda - \lambda^2}{\tau_P}$	-

3.2.1. Implementation of the Digital Form of PID Controller

The general continuous form of PID controller is given as shown in (11):

$$u(t) = K_p * [e(t) + \frac{1}{\tau_i} \int e(t)dt + \tau_d * \frac{de(t)}{dt}] \tag{11}$$

Implementation of a velocity form of PID controller [2] is shown in (12):

$$\Delta u(k) = q_0e(k) + q_1e(k - 1) + q_2e(k - 2) \tag{12}$$

$$q_0 = K_p \left(1 + \frac{\tau_d}{T_o} + \frac{T_o}{T_i} \right); \quad q_1 = -K_p \left(1 + 2\frac{\tau_d}{T_o} \right); \quad q_2 = K_p \left(\frac{\tau_d}{T_o} \right)$$

Several tuning algorithms are available for control systems based on that FO model, and, out of those, IMC is the preferred one. The tuning values of the IMC model are shown in Table 4.

3.2.2. Static Feedforward Control of PTC

In this section, static feedforward with a feedback controller is implemented to track the setpoint and to reject the measured disturbance. A schematic of manipulated and control variables along with disturbance is shown in Figure 7. The control variable for PTC control is to control the outlet HTFs' temperature by manipulating the HTF flow rate through PTC.

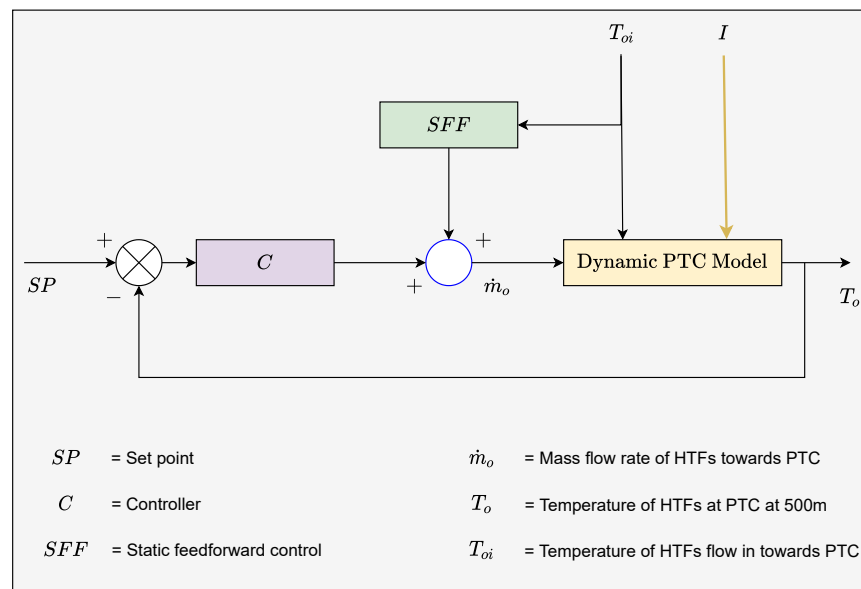


Figure 7. Control loop structure of PTC.

Static feedforward control of PTC is designed based on energy balance, and its result is obtained as shown in Equation (13). Then, it is combined with feedback PI control to obtain a resultant manipulated variable:

$$\begin{aligned} \dot{m}_{(o,FF)}(h_o - h_{oi}) &= IA\eta_{opt} \\ \dot{m}_{(o,FF)} &= \frac{IA\eta_{opt}}{(h_o - h_{oi})} \end{aligned} \tag{13}$$

where $\dot{m}_{(o,FF)}$, h_o , h_{oi} represent mass flow rate of HTFs, enthalpy of HTF fluid out of PTC, and enthalpy of HTF fluid flow towards the PTC, respectively. The enthalpy values are obtained as discussed in detail in Appendix A.

3.2.3. Performance Metrics of System

PTC in Closed Loop (CL) performance is characterized based on a few metrics such as Integral Absolute Error (IAE), Integral Squared Error (ISE), Integral Time Absolute Error (ITAE) and Integral Time Squared Error (ITSE), as shown in Table 5. Those metrics are obtained to characterize the tracking error residual.

Table 5. Performance metric of the controller.

Performance Metric ($e_{rr} = SP - PV$)	Expression
Integral Absolute Error (IAE)	$\int_0^{\infty} e_{rr} dt$
Integral Squared Error (ISE)	$\int_0^{\infty} e_{rr}^2 dt$
Integral Time Absolute Error (ITAE)	$\int_0^{\infty} t e_{rr} dt$
Integral Time Squared Error (ITSE)	$\int_0^{\infty} te_{rr}^2 dt$

4. Case Study of PTC with HTFs

Performance of PTC with different HTFs such as therminol oil, molten salt and water is evaluated with the following four case studies:

1. Constant solar radiation in open Loop (COL);
2. Constant solar radiation in closed loop (CCL);
3. Quadratic solar radiation in open loop (QOL);
4. Quadratic solar radiation in closed loop operation (QCL).

The performance of the case studied is evaluated by solar energy received (Q_{sr}) and the heat gain on PTC (Q_{th}), as shown in (15):

$$Q_{sr} = \int_{SPt} I(t)WL dt \quad (14)$$

$$Q_{th} = \int_{SPt} (h_o(t) - h_{oi}(t))\dot{m}_o(t) dt \quad (15)$$

where SPt stands for a time period of solar radiation applied for simulation as shown in Figure 8b. h_o and h_{oi} represent enthalpy of HTFs flow out of PTC and enthalpy of HTFs flow in, respectively.

Solar radiation and temperature of therminol oil/molten salt flowing in towards PTC for this respective case study are shown in Figure 8a,b. Figure 9 shows that the temperature of water flowing in towards PTC is shown with similar solar radiation, which is applied as shown in Figure 8b. In the case study of quadratic solar radiation, a disturbance in solar radiation is affected at the leading edge of 2 h and trailing edge of 6 h, respectively, and the corresponding radiation decreases by 65% and 68%, respectively. In CCL and QCL case studies, in the first one hour of operation, PTC is simulated in open-loop operation with constant values of MV, and then control action is activated after 1 h of operation. The performance metrics of the controller for PTC case studies are discussed in Table 6. These metrics show the controller performance for the simulation period, and the corresponding setpoints are updated every two hours.

Table 6. PTC Controller performance on case studies.

Controller Performance		PTCTHO	PTCMS	PTCWAT
CCL	IAE	4.31×10^4	2.94×10^4	1.041×10^4
	ISE	1.06×10^6	3.48×10^5	6.20×10^5
	ITSE	1.18×10^8	1.37×10^8	1.27×10^6
	ITASE	1.059×10^9	1.032×10^9	6.97×10^7
QCL	IAE	7.66×10^4	1.66×10^5	1.31×10^4
	ISE	1.71×10^6	2.89×10^6	8.56×10^5
	ITSE	5.48×10^8	1.65×10^9	1.95×10^6
	ITASE	5.52×10^9	1.92×10^{10}	1.10×10^8

The Process Variable (PV) performance of HTFs for case studies is shown in Figures 10–12, whereas the Manipulated Variable (MV) variation of HTFs for case studies is shown in Figures 13–15.

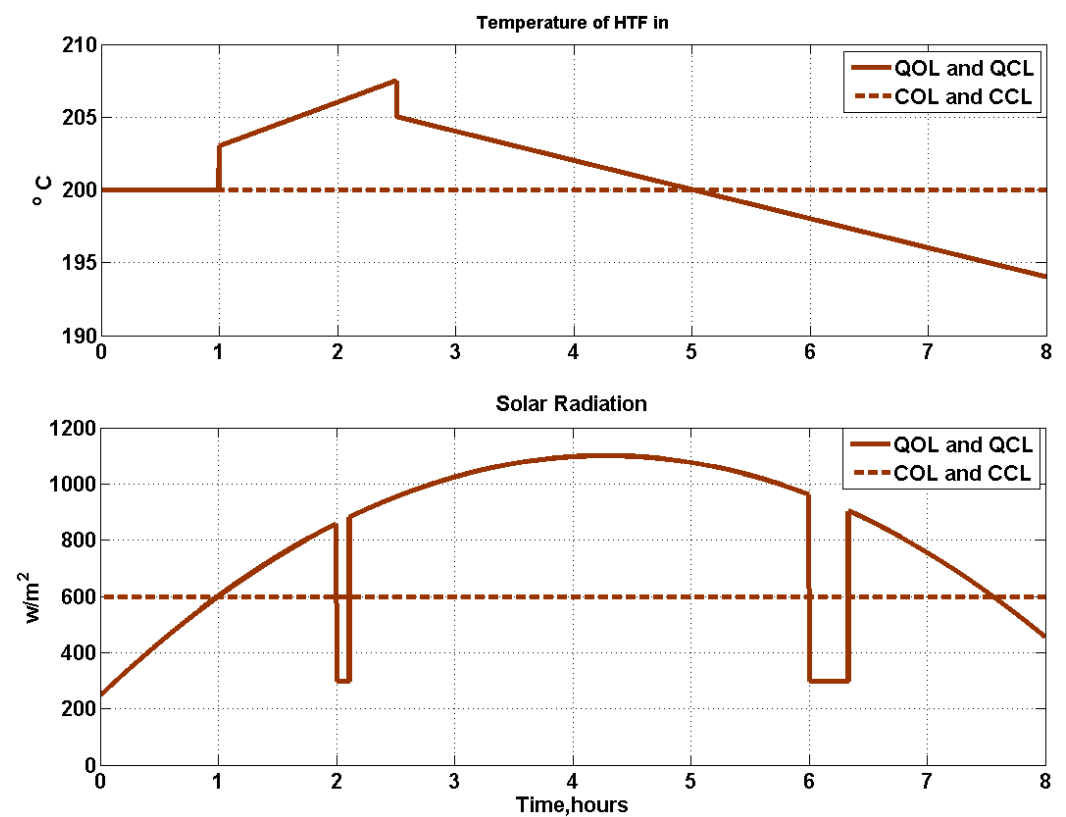


Figure 8. (a) Temperature of therminol oil/molten salt flowing in towards PTC; (b) solar radiation applied for case studies.

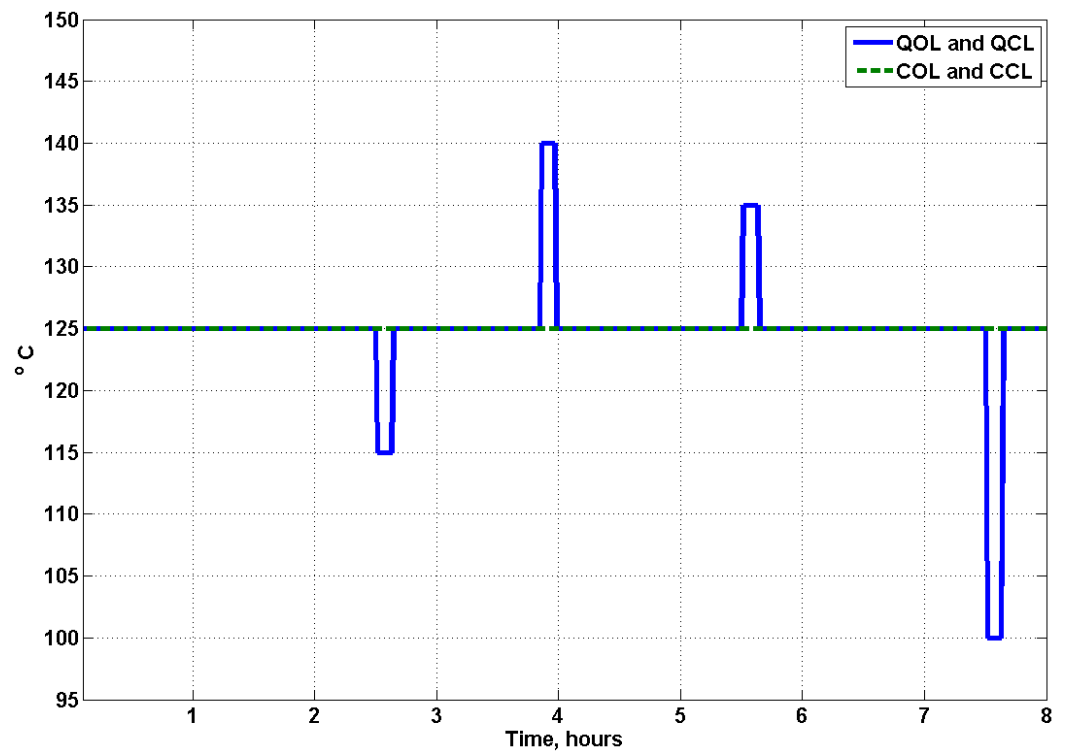


Figure 9. Temperature of water input to PTC.

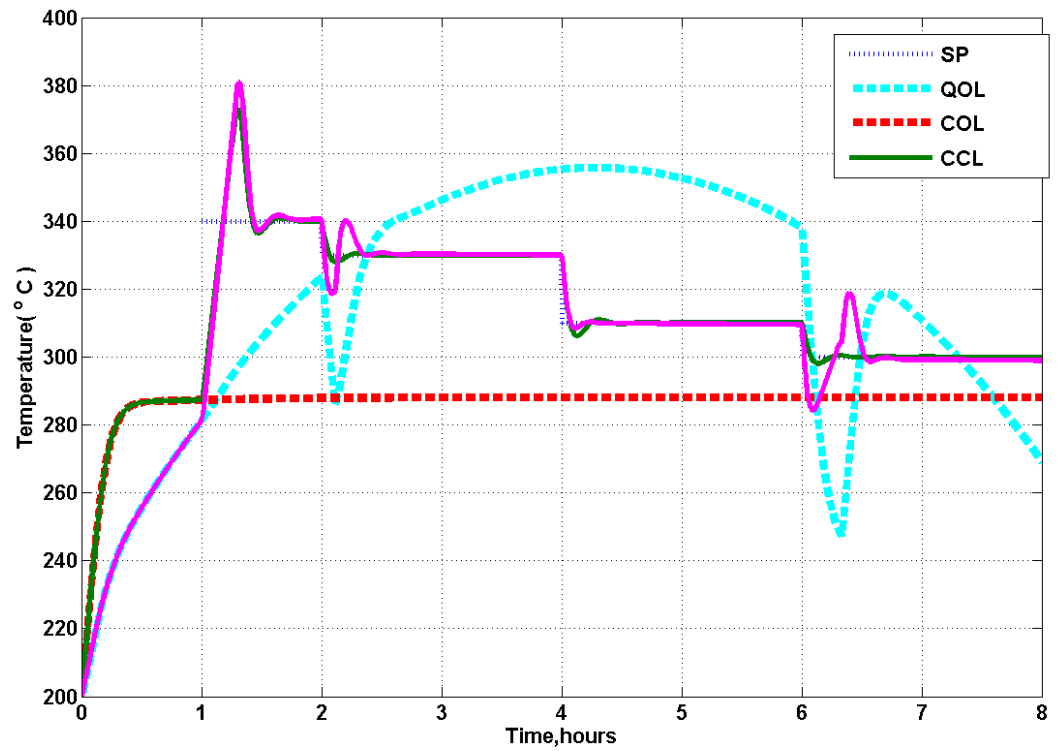


Figure 10. Process variables (PV) of therminol oil.

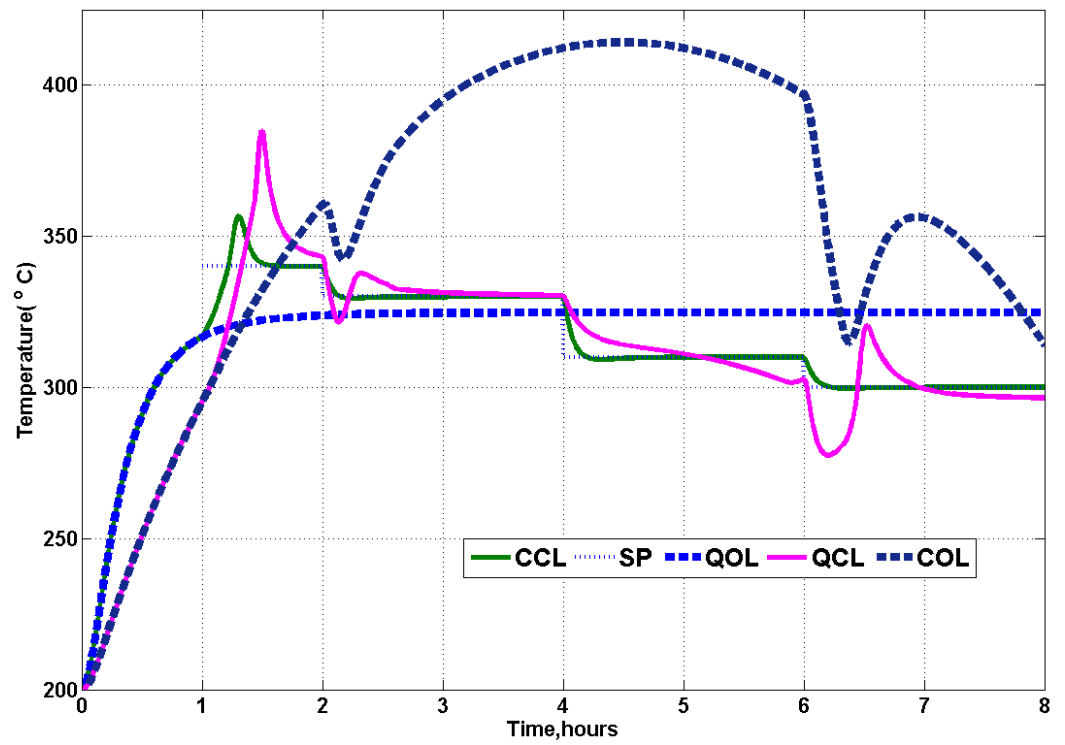


Figure 11. Process variables (PV) of molten salt.

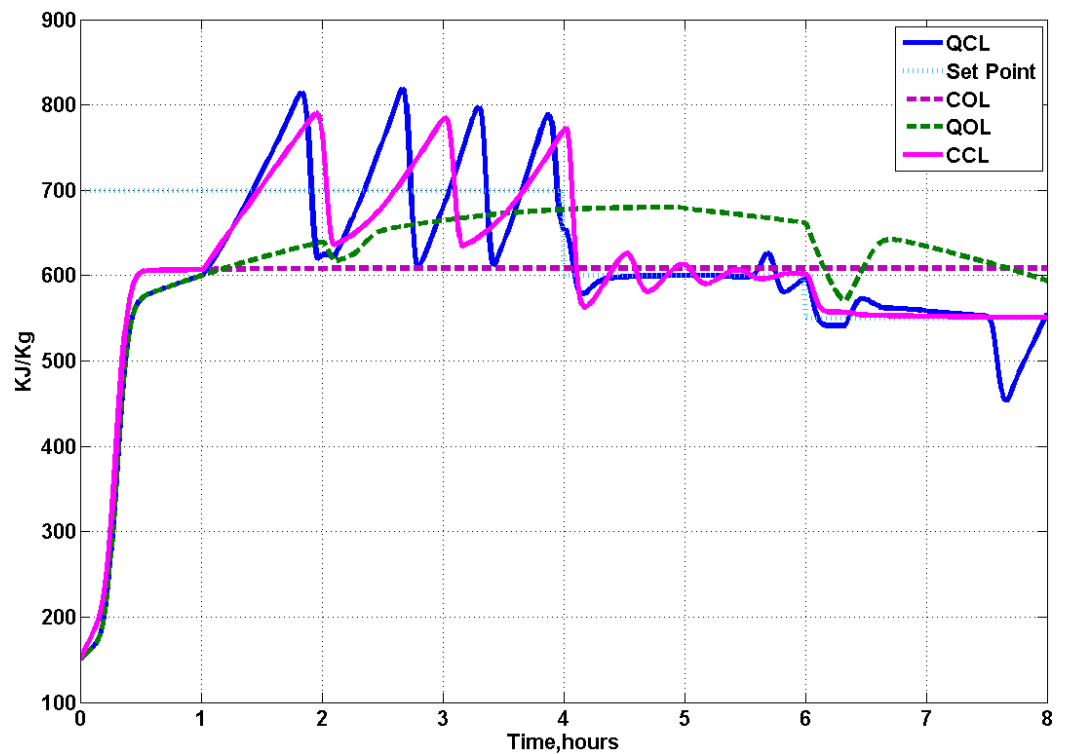


Figure 12. Enthalpy of process variables (PV) of water.

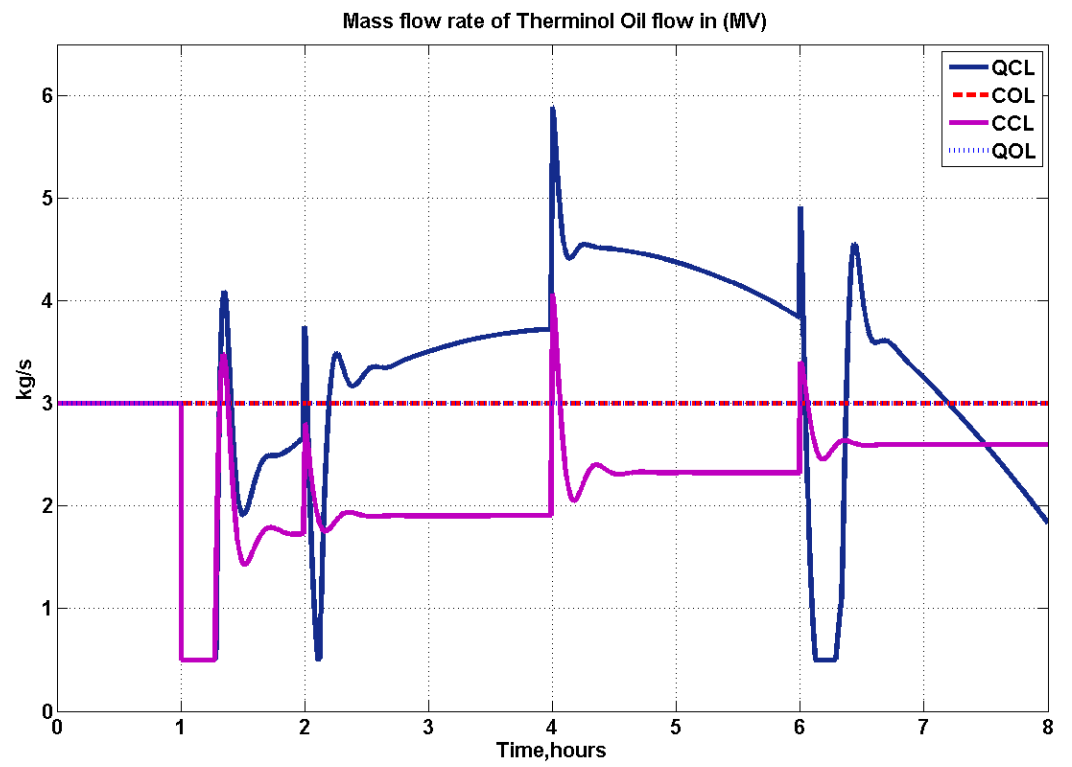


Figure 13. Manipulated variables (MV) of therminol oil.

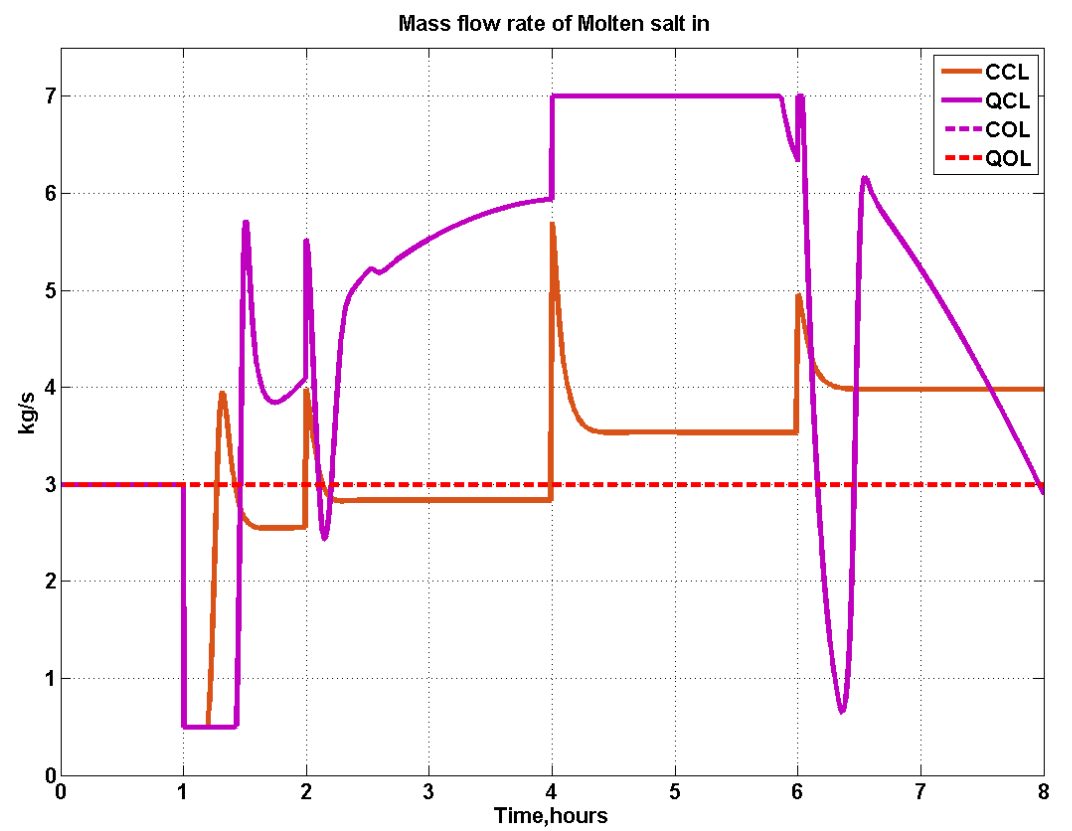


Figure 14. Manipulated variables (MV) of molten salt.

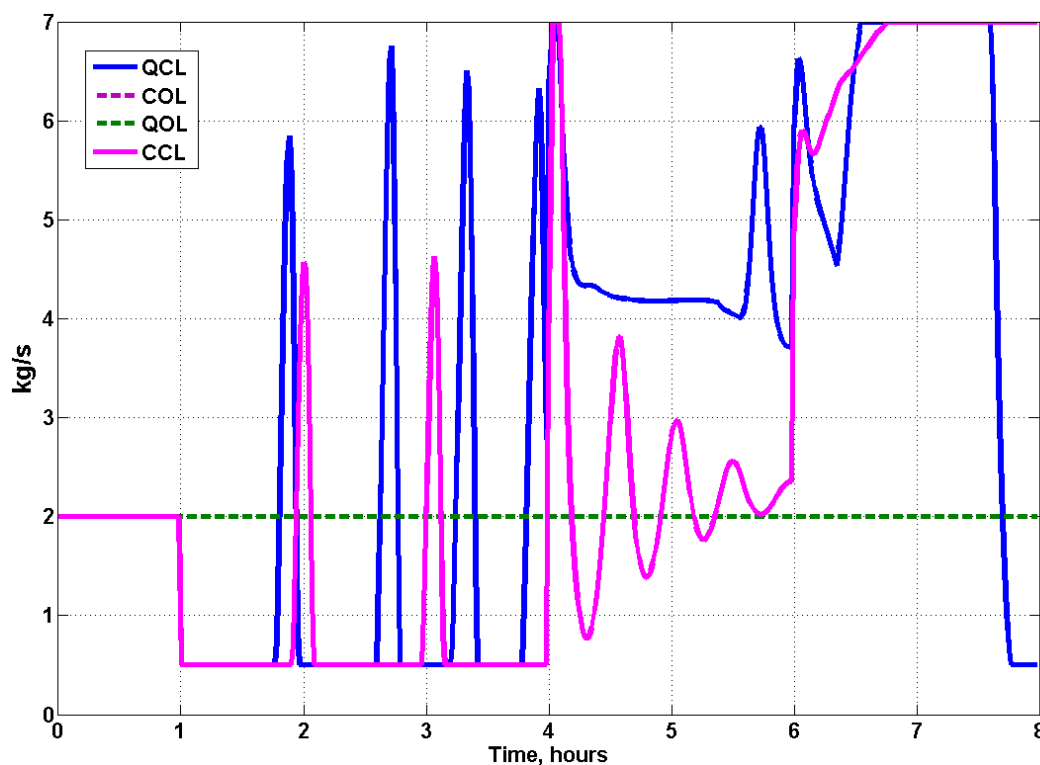


Figure 15. Enthalpy of manipulated variables (MV) of water.

4.1. Constant Solar Radiation with Open Loop Operation (COL)

Table 7 shows the values of Steady State (SS), initial, MV, and PV variations during solar variation. Time taken for HTFs to reach SS is about 30 min, 1 h, 31 min and 36 min, respectively. For COL, the solar energy received is 19,906 MJ, and the collected thermal energy for therminol oil, molten salt, and water is 16,277, 14,678, and 3733 MJ, respectively. Its corresponding performance analysis is shown in Table 8. Therminol oil collects more energy compared to molten salt and water at an efficiency of 81%, whereas, for molten salt and water, it has the efficiency of 73% and 18.7%, respectively.

Table 7. Control parameters performance for case studies. (Abbreviations used in this table are: THO = Therminol oil, MS = Molten salt, WAT = Water, LE = Leading edge at 2 h, TE = Trailing edge at 6 h, PV: Process variable, MV = Manipulated variable, SSPV = Steady State value of PV, SSMV = Steady State value of MV, PV_{MAX} = Maximum value of PV.)

		SSPV (°C)	PVM _{Max} (°C)	Temperature of HTF at 0, 4, 8 h (°C)	PV Variation Due to Solar Disturbance (°C)		MV Variation Due to Solar Disturbance (Kg/S)	
					LE	TE	LE	TE
COL	THO	288	288	200, 288, 288	-	-	-	-
	MS	324	324	200, 324, 324	-	-	-	-
	WAT	114	114	35, 144, 144	-	-	-	-
CCL	THO	-	372	200, 288, 288	-	-	-	-
	MS	-	356	200, 330, 296	-	-	-	-
	WAT	-	184	35, 184, 130	-	-	-	-
QOL	THO	-	355	200, 355, 269	323 to 286	338 to 247	SSMV: 3	SSMV: 3
	MS	-	414	200, 412, 315	360 to 342	396 to 352	SSMV: 3	SSMV: 3
	WAT	-	160	35, 160, 141	150 to 146	156 to 135	SSMV: 2	SSMV: 2
QCL	THO	-	380	200, 355, 269	323 to 286	308 to 284	3 to 0.512	4 to 6.5
	MS	-	384	200, 330, 315	340 to 322	302 to 277	5.52 to 2.43	7 to 6.5
	WAT	-	192	35, 144, 128	148 to 147	138 to 128	0.5 to 0.5	6.5 to 4.5

4.2. Constant Solar Radiation with Closed Loop Operation (CCL)

For the proposed CCL, the solar energy received is 19,906 MJ. The collected thermal energy for therminol oil, molten salt, and water is 15,845, 15,040, and 3892 MJ, respectively, and its performance analysis is shown in Table 8. Therminol oil collects more energy compared to molten salt and water; it is at an efficiency of 79%. However, for molten salt and water, it has the efficiency of 75% and 19%, respectively.

4.3. Quadratic Solar Radiation with Closed Loop Operation (QOL)

For the QOL, the solar energy received is 26,989 MJ. The collected thermal energy for therminol oil, molten salt, and water is 22,210, 19,456, and 5450 MJ, respectively, and its performance analysis is shown in Table 8. Therminol oil collects more energy compared to molten salt and water; it is at an efficiency of 82%, whereas, for molten salt and water, it has the efficiency of 72% and 20%, respectively.

In Leading Edge (LE) of disturbances (2 h), the temperature varies by about 31 °C for therminol oil. Furthermore, in the case of molten salt and water, it is about 18 and 4 °C, respectively. In the Trailing Edge (TE) of disturbances (6 h), temperature varies by about 91 °C for therminol oil, and, in the case of molten salt and water, it is about 81 and 21 °C, respectively.

4.4. Quadratic Solar Radiation with Closed Loop Operation (QCL)

Solar energy received for the QCL is 26,989 MJ, and collected thermal energy for therminol oil, molten salt and water is 22,256, 22,101, and 5712 MJ, respectively. Furthermore, its performance analysis is shown in Table 8. Therminol oil collects more energy compared to molten salt and water; it is at an efficiency of 82%, whereas, for molten salt and water, it has the efficiency of 81% and 21%, respectively.

In LE of disturbances (2 h), temperature varies by about 31 °C for therminol oil, and, in the case of molten salt and water, it is about 18 and 4 °C, respectively. In TE, temperature varies by about 91 °C for therminol oil. In the case of molten salt and water, it is about 81 °C and 21 °C, respectively.

Table 8. PTC case studies' performance.

		PTCTHO	PTCMS	PTCWAT
Solar energy collected Q_{sr} (MJ)	COL	-	19,906	-
	QOL		26,989	
	CCL	-	19,906	-
	QCL		26,989	
Thermal energy extracted Q_{th} (MJ)	COL	16,277	14,678	3733
	QOL	22,210	19,456	5450
	CCL	15,845	15,040	3892
	QCL	22,256	22,101	5712

PTCTHO = PTC with therminol oil; PTCMS = PTC with molten salt; PTCWAT = PTC with water.

5. Conclusions

In this paper, the performance of PTC with HTF of therminol oil, molten salt and water is analyzed with different case studies, and its main outcomes are summarized as follows:

- With constant solar radiation of 600 W/m² for an 8-hour duration, solar energy collected was about 19,906 MJ. Based on this condition, the open-loop performance showed higher heat gain collected by therminol oil with an improvement by 16,277 MJ, i.e., 81%, whereas molten salt and water collected with 14,678 MJ and 3733 MJ, respectively.
- In a quadratic solar radiation case study, the solar energy collected about 26,989 MJ; open-loop performance had a higher heat gain collected by therminol oil by approxi-

mately 22,210 MJ, i.e., 82%, whereas molten salt and water collected with 19,456 MJ and 5450 MJ, respectively.

- In the closed-loop performance with the designed PI controller, therminol oil performance showed better tracking and disturbance rejection. With constant solar disturbances, molten salt showed better performance, whereas, in the case of disturbance of solar radiation, the tracking and disturbance reaction of PTC with molten salt is not adequate.
- During intermittent solar radiation, temperature variation with therminol oil is affected by 91 °C, whereas molten salt and water becomes affected by 44 °C and 21 °C, respectively.
- Heat gain captured by water as HTF is less compared to therminol oil and molten salt. For four case studies, it is in a range of about 18.7 to 21.6%. The oscillations of water flow rate as MV are more compared to therminol oil and molten salt.

Based on the open and closed-loop operation of PTC with different HTF, proper HTF can be selected based on cost and operational complexity. This study sets the benchmark problem for PTC in both open and closed-loop with different HTF such as therminol oil, molten salt, and water. Advance controller design technique and optimization based control with plant constraints are the future scope of this article.

Author Contributions: Conceptualization, S.K. and N.D.B.; methodology, S.K. and N.D.B.; software, S.K. and N.D.B.; validation, S.K. and N.D.B.; formal analysis, S.K. and N.D.B.; investigation, S.K. and N.D.B.; resources, S.K. and N.D.B.; data curation, S.K. and N.D.B.; writing—original draft preparation, S.K. and N.D.B.; writing—review and editing, S.K. and N.D.B.; visualization, S.K. and N.D.B.; supervision, S.K. and N.D.B.; project administration, S.K. and N.D.B.; funding acquisition, S.K. and N.D.B. All authors have read and agreed to the published version of the manuscript.

Funding: This research received no external funding.

Institutional Review Board Statement: Not applicable.

Informed Consent Statement: Not applicable.

Data Availability Statement: The data presented in this study are available on request from the corresponding author.

Conflicts of Interest: The authors declare no conflict of interest.

Abbreviations

The following abbreviations are used in this manuscript:

PTC	Parabolic Trough Collector
HTF	Heat Transfer Fluid
HTFs	Heat Transfer Fluids of therminol oil/molten salt/ water
ODEs	Ordinary Differential Equations
PDEs	Partial Differential Equations
SCF	Solar Collector Field
PV	Process Variable
MV	Manipulated Variable
COL	Constant Solar Radiation with Open Loop Operation
CCL	Constant Solar Radiation with Closed Loop Operation
QOL	Quadratic Solar Radiation with Open Loop Operation
QCL	Quadratic Solar Radiation with Closed Loop Operation
PTCTHO	Parabolic Trough Collector with therminol oil as heat transfer fluid
PTCMS	Parabolic trough collector with molten salt as heat transfer fluid
PTCWAT	Parabolic trough collector with water as heat transfer fluid

Appendix A. Heat Transfer Fluid

Appendix A.1. Therminol Oil

Variation of properties of therminol oil with temperature ($^{\circ}\text{C}$) is presented as follows [33]:

$$\begin{aligned} \text{Density (kg/m}^3\text{)} &= -0.90797T + 0.00078116T^2 \\ &\quad - 2.367 \times 10^{-6}T^3 + 1083.25 \\ \text{Specific heat capacity (kJ/kg} \cdot \text{K)} &= 0.002414T + 5.9591 \times 10^{-6}T^2 \\ &\quad - 2.9879 \times 10^{-8}T^3 \\ &\quad + 4.4172 \times 10^{-11}T^4 + 1.498 \\ \text{Thermal conductivity (W/m} \cdot \text{K)} &= -8.19477 \times 10^{-5}T - 1.92257 \times 10^{-7}T^2 \\ &\quad + 2.5034 \times 10^{-11}T^3 \\ &\quad - 7.2974 \times 10^{-15}T^4 + 0.137743 \\ \text{Enthalpy (}f_h\text{)(kJ/kg)} &= -18.17 + 1.496T - 0.000147T^2 \\ \text{Kinematic viscosity (mm}^2\text{/s)} &= e^{\left(\frac{544.149}{T+114.43} - 2.59578\right)} \end{aligned}$$

where T is the therminol oil temperature ($^{\circ}\text{C}$).

Out of these relationships, the equations for the temperature dependence of density, specific heat capacity, thermal conductivity, and kinematic viscosity were directly taken from the Solutia report [33], and the temperature dependence of enthalpy was obtained by fitting a second-degree polynomial to temperature–enthalpy data obtained from the Solutia report [33].

Appendix A.2. Molten Salt [34]

$$\begin{aligned} \text{Density (kg/m}^3\text{)} &= 2090 - 0636T \\ \text{Specific heat capacity (kJ/kg} \cdot \text{K)} &= 1443 - 0.172T \\ \text{Thermal conductivity (W/m} \cdot \text{K)} &= 0.443 + 1.9 \times 10^{-4}T \\ \text{Kinematic viscosity (kg/ms)} &= (22.71 - 0.12T + 22.281 \times T^2) \times 10^{-3} \end{aligned}$$

Appendix A.3. Water

Thermodynamic properties of water and steam are accessed from MATLAB library files Xsteam [30].

Appendix B. Single Phase Convective Heat Transfer Coefficient (h_p)

A single phase convective heat transfer coefficient for working fluid is obtained as follows [15]:

$$h_p = 0.023R_e^{0.8}P_r^{0.4}\frac{K}{D_a} \quad (\text{A1})$$

where the Reynolds number and Prandtl number are computed as

$$\text{Reynolds number } R_e = \frac{D_a u}{\nu}, \quad \text{Prandtl number } P_r = \frac{\nu \rho C_p}{K}$$

Appendix C. Solar Energy Received per Unit Volume on Absorber Pipe for Sectional Length (PTCWAT)

The term q_w in energy equation is linked with solar energy received per unit volume on absorber pipe for sectional length and is computed as:

$$q_w = \frac{Q_{heat}}{(\pi r_{Ao}^2 \Delta x)} \quad (A2)$$

$$\text{where } Q_{heat} = h_{(p,LFR)} A_A (T_A - T_{(w/st/2\phi)})$$

The heat transfer coefficient $h_{(p,LFR)}$ may be $h_{(p,1\phi)}$ or $h_{2\phi}$ depending on the working fluid condition such as a single-phase and two-phase condition, respectively. The computation of these heat transfer coefficients is discussed in Section 2.2. Furthermore, $T_{(w/st/2\phi)}$ represents temperature of working fluid, Δx is the distance between two grid points in the finite difference approximation, and Δt is the time step.

Appendix D. Case Study of PTCWAT for Steam Quality ($QOL_{(stq)}$)

A current case study is performed to realize the DSG from PTC, which results in pressure drops more compared to the input side of PTC, and the enthalpy of water varies where the temperature is constant. This is similar to that of the case study discussed of QOL , where the difference between QOL and $QOL_{(stq)}$ and the optical efficiency increased while maintaining the $\eta_{opt} = 0.75$. The temperature of water flowing is maintained at 200 °C with a mass flow rate of water at 1.5 kg/s. Based on these parameter variations, the temperature of water/steam exiting out of PTC at 500 m is shown in Figure A1a. Even though the temperature is constant at 2.5 to 6 h, the variation in enthalpy occurs. The profile of enthalpy water/steam exiting out of PTC at 500 m is shown in Figure A1b, and the profile of steam quality exit at PTC (Figure A1c). Once the steam is generated in PTC, there is a pressure variation of 0.63 bar as shown in Figure A1d. At 250 m, there is no steam generation, and the pressure drop is 0.17 bar.

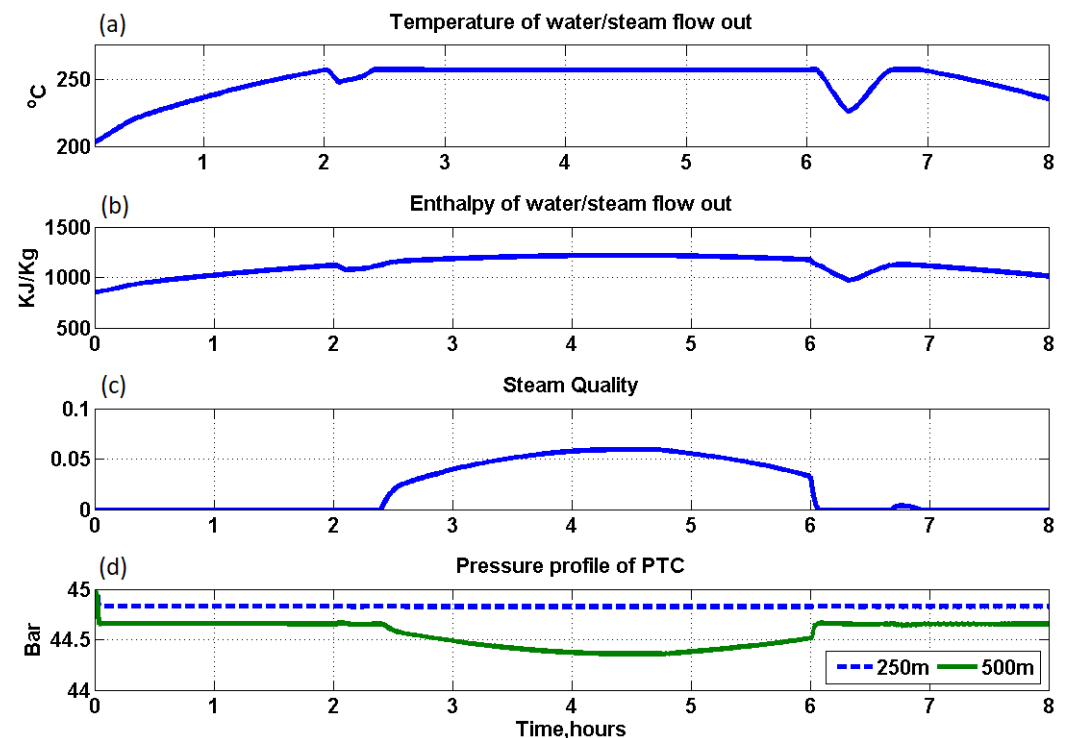


Figure A1. PTCWAT profile $QOL_{(stq)}$: (a) temperature of water/steam at 500 m; (b) enthalpy of water/steam at 500 m; (c) steam quality at 500 m; (d) pressure variation at 250 m and 500 m.

Appendix E. Transfer Function Fit Percentage

The best fit model is obtained by minimizing the error between predicted and measured value from the PTC. The corresponding percentage fit of a transfer function is obtained by Equation (A3) [35]:

$$Ft_{TF} = \left(1 - \frac{\sum_{i=1}^{t_p} |Ym_i - \widetilde{Y}_{s_i}|}{\sum_{i=1}^{t_p} |Ym_i - \overline{Ym}|} \right) \times 100 \quad (\text{A3})$$

In the above equation, \widetilde{Y}_{s_i} represents the predicted (fitted) model output at time instant i . Ym_i, \overline{Ym} represents output measured from the plant at time instant i and the mean value of measured output, respectively. The data are collected for t_p instants with a sampling interval of 1 s. The transfer functions identified for various subsystems and the corresponding fit errors (Equation (A3)) are listed in Table 3. It can be seen from this table that transfer functions fit the data quite well for most of the subsystems.

Table A1. LFR: notation and values of parameters (Equations (4) to (9)).

Symbol	Description	Units	Values
$T_{(w/st/2\phi)}$	Temperature of water/steam/ two phase mixture depending on operating condition	$^{\circ}\text{C}$	
ρ	Density of working fluid	kg/m^3	
h	Specific enthalpy of working fluid	J/kg	
q	Quality of steam		
u	Velocity flow velocity of working fluid	m/s	
P	Pressure	bar	
C_k	Friction constant		
q_w	Heat per unit volume of flow (refer (A2))	W/m^3	
A_A, A_E	Cross-sectional area: absorber pipe and glass envelope	m^2	$1.9 \times 10^{-3}, 2.8 \times 10^{-3}$
C_A, C_E	Specific heat capacity: absorber pipe and glass envelope	$\text{J}/\text{kg}/\text{K}$	460 [8], 840 [8], Function of temperature
h_{air}, h_p	Convective heat transfer coefficient air–glass envelope, HTC of working fluid	$\text{W}/(\text{m}^2 \text{ } ^{\circ}\text{C})$	25, refer to section S.2.2.2 [19]
I	Solar radiation incident on PTC collector surface	W/m^2	
L	Length of PTC	m	500
T_A, T_E	Temperature: absorber pipe, and glass envelope	$^{\circ}\text{C}$	Variable
T_{air}, T_{sky}	Temperature: Ambient, effective sky temperature	$^{\circ}\text{C}$	25, 40
W	Width of mirror aperture	m	14
ξ_A, ξ_E	Emissivity: absorber pipe and glass envelope		0.18, 0.9
η_{opt}	Total optical efficiency of PTC	–	0.4
σ	Stefan–Boltzmann constant	$\text{W}/(\text{m}^2\text{K}^4)$	5.67×10^{-8}
g	Gravitational acceleration	m/s^2	9.8
μ_l	Liquid dynamic viscosity	$\text{kg}/(\text{ms})$	
μ_g	Steam dynamic viscosity	$\text{kg}/(\text{ms})$	
μ_{fg}	Viscosity difference between liquid and steam	$\text{kg}/(\text{ms})$	
f_f	Pipe friction constant		

References

1. Kalogirou, S.A. Solar thermal collectors and applications. *Prog. Energy Combust. Sci.* **2004**, *30*, 231–295. [CrossRef]
2. Stephanopoulos, G. *Chemical Process Control*; Prentice Hall: Upper Saddle River, NJ, USA, 1984; Volume 2.
3. Tagle-Salazar, P.D.; Nigam, K.D.; Rivera-Solorio, C.I. Parabolic trough solar collectors: A general overview of technology, industrial applications, energy market, modeling, and standards. *Green Process. Synth.* **2020**, *9*, 595–649. [CrossRef]
4. Camacho, E.F.; Berenguel, M. Control of solar energy systems. *IFAC Proc. Vol.* **2012**, *45*, 848–855. [CrossRef]

5. Desai, N.B.; Bandyopadhyay, S.; Nayak, J.K.; Banerjee, R.; Kedare, S.B. Simulation of 1MWe solar thermal power plant. *Energy Procedia* **2014**, *57*, 507–516. [[CrossRef](#)]
6. Saucedo, D.; Velázquez, N.; Beltrán, R.; Luna, A. Comparative Analysis Between a Parabolic Trough Collector and a Compact Linear Fresnel Reflector To Be Used As Direct Generator of an Advanced Absorption Cooling System. *Adv. Appl. Mech. Eng. Technol.* **2010**, *2*, 1–18.
7. Camacho, E.F.; Rubio, F.R.; Berenguel, M.; Valenzuela, L. A survey on control schemes for distributed solar collector fields. Part II: Advanced control approaches. *Sol. Energy* **2007**, *81*, 1252–1272. [[CrossRef](#)]
8. Powell, K.M.; Edgar, T.F. Modeling and control of a solar thermal power plant with thermal energy storage. *Chem. Eng. Sci.* **2012**, *71*, 138–145. [[CrossRef](#)]
9. Kannaiyan, S.; Bhartiya, S.; Bhushan, M. Dynamic Modeling and Simulation of a Hybrid Solar Thermal Power Plant. *Ind. Eng. Chem. Res.* **2019**, *58*, 7531–7550. [[CrossRef](#)]
10. Nayak, J.K.; Kedare, S.B.; Banerjee, R.; Bandyopadhyay, S.; Desai, N.B.; Paul, S.; Kapila, A. A 1 MW national solar thermal research cum demonstration facility at Gwalpahari, Haryana, India. *Curr. Sci.* **2015**, *109*, 1445–1457. [[CrossRef](#)]
11. Silva, R.N.; Rato, L.M.; Lemos, J.M. Time scaling internal state predictive control of a solar plant. *Control Eng. Pract.* **2003**, *11*, 1459–1467. [[CrossRef](#)]
12. Camacho, E.F.; Berenguel, M.; Rubio, F.R. *Advanced Control of Solar Plants*; Advances in Industrial Control; Springer: London, UK, 1997. [[CrossRef](#)]
13. Pin, G.; Falchetta, M.; Fenu, G. Adaptive time-warped control of molten salt distributed collector solar fields. *Control Eng. Pract.* **2008**, *16*, 813–823. [[CrossRef](#)]
14. Chatoorgoon, V. SPORTS—A simple nonlinear thermohydraulic stability code. *Nucl. Eng. Des.* **1986**, *93*, 51–67. [[CrossRef](#)]
15. Yan, Q.; Hu, E.; Yang, Y.; Zhai, R. Dynamic modeling and simulation of a solar direct steam-generating system. *Int. J. Energy Res.* **2010**, *34*, 1341–1355. [[CrossRef](#)]
16. Pye, J.D.; Morrison, G.L.; Behnia, M. Unsteady effects in direct steam generation in the CLFR. In *Proceedings of the ANZSES Solar Conference*; Australian and NZ Solar Energy Society: Frenchs Forest, NSW, Australia, 2007; Volume 10, p. 02-2007.
17. Eck, M.; Hirsch, T. Dynamics and control of parabolic trough collector loops with direct steam generation. *Sol. Energy* **2007**, *81*, 268–279. [[CrossRef](#)]
18. Hirsch, T.; Steinmann, W.; Eck, M. Simulation of transient two-phase flow in parabolic trough collectors using Modelica. In *Proceedings of the 4th International Modelica Conference*, Hamburg-Harburg, Germany, 7–8 March 2005; pp. 1–11.
19. Odeh, S.D.; Morrison, G.L.; Behnia, M. Modelling of parabolic trough direct steam generation solar collectors. *Sol. Energy* **1998**, *62*, 395–406. [[CrossRef](#)]
20. Zima, W.; Cisek, P.; Cebula, A. Mathematical model of an innovative double U-tube sun-tracked PTC and its experimental verification. *Energy* **2021**, *235*, 121293. [[CrossRef](#)]
21. Norouzi, A.M.; Siavashi, M.; Ahmadi, R.; Tahmasbi, M. Experimental study of a parabolic trough solar collector with rotating absorber tube. *Renew. Energy* **2021**, *168*, 734–749. [[CrossRef](#)]
22. Cirre, C.M.; Berenguel, M.; Valenzuela, L.; Klempous, R. Reference governor optimization and control of a distributed solar collector field. *Eur. J. Oper. Res.* **2009**, *193*, 709–717. [[CrossRef](#)]
23. Ferruzza, D.; Topel, M.; Basaran, I.; Laumert, B.; Haglind, F. Start-up performance of parabolic trough concentrating solar power plants. In *Proceedings of the AIP Conference Proceedings*; AIP Publishing LLC: New York, NY, USA, 2017; Volume 1850, p. 160008.
24. Kannaiyan, S.; Bhartiya, S.; Bhushan, M. Plantwide Decentralized Controller Design for Hybrid Solar Thermal Power Plant. *Front. Control Eng.* **2022**, *3*, 853625. [[CrossRef](#)]
25. Camacho, E.; Rubio, F.; Berenguel, M.; Valenzuela, L. A survey on control schemes for distributed solar collector fields. Part I: Modeling and basic control approaches. *Sol. Energy* **2007**, *81*, 1240–1251. [[CrossRef](#)]
26. Barcia, L.; Peón Menéndez, R.; Martínez Esteban, J.; José Prieto, M.; Martín Ramos, J.; de Cos Juez, F.; NevadoReviriego, A. Dynamic modeling of the solar field in parabolic trough solar power plants. *Energies* **2015**, *8*, 13361–13377. [[CrossRef](#)]
27. Kannaiyan, S.; Bokde, N.D.; Geem, Z.W. Solar Collectors Modeling and Controller Design for Solar Thermal Power Plant. *IEEE Access* **2020**, *8*, 81425–81446. [[CrossRef](#)]
28. Valenzuela, L.; Zarza, E.; Berenguel, M.; Camacho, E.F. Control concepts for direct steam generation in parabolic troughs. *Sol. Energy* **2005**, *78*, 301–311. [[CrossRef](#)]
29. Arousseau, A.; Vuillerme, V.; Beziau, J.J. Control systems for direct steam generation in linear concentrating solar power plants—A review. *Renew. Sustain. Energy Rev.* **2016**, *56*, 611–630. [[CrossRef](#)]
30. Holmgren, M. X Steam—Thermodynamic Properties of Water and Steam. Available online: <https://www.mathworks.com/matlabcentral/fileexchange/9817-x-steam-thermodynamic-properties-of-water-and-steam> (accessed on 1 September 2018).
31. Bequette, B.W. *Process Control: Modeling, Design, and Simulation*; Prentice Hall Professional: Upper Saddle River, NJ, USA, 2003.
32. Rivera, D.E. *Internal Model Control: A Comprehensive View*; Arizona State University: Tempe, AZ, USA, 1999; pp. 85287–6006.
33. SOLUTIA. Properties of Therminol VP-1 vs Temperatures-Liquid Phase. Available online: <http://twf.mpei.ac.ru/tthb/hedh/htf-vp1.pdf> (accessed on 1 September 2018).

-
34. Chang, Z.; Li, X.; Xu, C.; Chang, C.; Wang, Z. The design and numerical study of a 2MWh molten salt thermocline tank. *Energy Procedia* **2015**, *69*, 779–789. [[CrossRef](#)]
 35. Wibowo, T.C.S.; Saad, N.; Karsiti, M.N. System identification of an interacting series process for real-time model predictive control. In Proceedings of the 2009 American Control Conference, St. Louis, MO, USA, 10–12 June 2009; pp. 4384–4389.